Full Paper Transactions, SMiRT 28
Toronto, Canada, August 10-15, 2025

PUSHOVER ANALYSIS AND CONCEPTUAL DESIGN OF RC FRAMES-CHALLENGES IN SEISMIC DESIGN FOR NUCLEAR FACILITIES

J. I. Ezeberry Parrotta[1], G. Hanna[2], D. Combescure[3]

[1] Technical Lead, IDOM, Madrid, Spain (jezeberry@idom.com)
[2] Technical Officer, Fusion for Energy (F4e), European Commission, Barcelona, Spain (Gaston.Hanna@f4e.europa.eu)
[3] Technical Officer, Fusion for Energy (F4e), European Commission, Barcelona, Spain (Didier.Combescure@f4e.europa.eu)

ABSTRACT

This paper presents a detailed nonlinear static pushover analysis for reinforced concrete (RC) frame structures, focusing on seismic design challenges specific to ITER facilities. The analysis explores the interplay among structural irregularities, high reinforcement demands, and geometrical constraints imposed by existing underground services. Capacity curves, behavior factors (q), and plastic hinge formation are evaluated using advanced computational methods.

The study focuses on two structures, Building #18 (on soft soil) and Building #20 (on rock), identifying significant differences in reinforcement requirements and effective ductility. Solutions such as optimized beam dimensions and enhanced foundation systems are implemented to address excessive reinforcement and ductility demands. The results show that actual behavior factors are slightly lower than assumed values, yet performance points remain safely distant from collapse thresholds.

The findings underscore the necessity of limiting the behavior factor to a maximum value of 2 for structures with similar constraints. This conservative approach ensures resilience and compliance with seismic performance criteria, offering valuable insights for the conceptual design of the ITER facilities in high-seismic zones.

INTRODUCTION

The ITER project is continually evolving, requiring new facilities to be constructed over existing structures and services. This situation imposes significant geometrical constraints—such as the presence of underground galleries and critical services—that can be difficult to accommodate. Although these facilities are not necessarily safety-related, their potential collapse during seismic events could cause damage to safety-related structures and components, necessitating careful design.

The purpose of this paper is to present the methodology followed for the conceptual design of new reinforced concrete (RC) buildings in the ITER project under seismic loads. The classical approach based on linear-elastic analyses is complemented by the recommendations of Eurocode 8, which permits the use of the "Behavior Factor" concept. This approach allows a reduction in seismic loads proportional to the structure's ductility. While this methodology is well established in current practice, its application to nuclear facilities requires particular attention. The unique challenges posed by nuclear sites—such as strict performance criteria and geometrical constraints—often demand substantial reinforcement to meet ultimate limit state (ULS) requirements.

The analysis in this paper focuses on Buildings #18 and #20, whose dimensions are presented in Figure 1. These buildings have distinct foundation conditions—soft soil for Building #18 and rock for Building #20—adding complexity to the design. The analysis evaluates the structural response under seismic loads, focusing on ductility, stability, and reinforcement requirements in compliance with Eurocode 8. By addressing these aspects, the study aims to ensure both safety and structural integrity during seismic events.

Additionally, the findings provide critical insights for refining design decisions and improving seismic resilience. By incorporating considerations such as load combinations, soil-structure interaction, and nonlinear behavior, this work lays the groundwork for advancing conceptual design strategies in high-seismic zones, particularly for critical facilities like those at ITER.

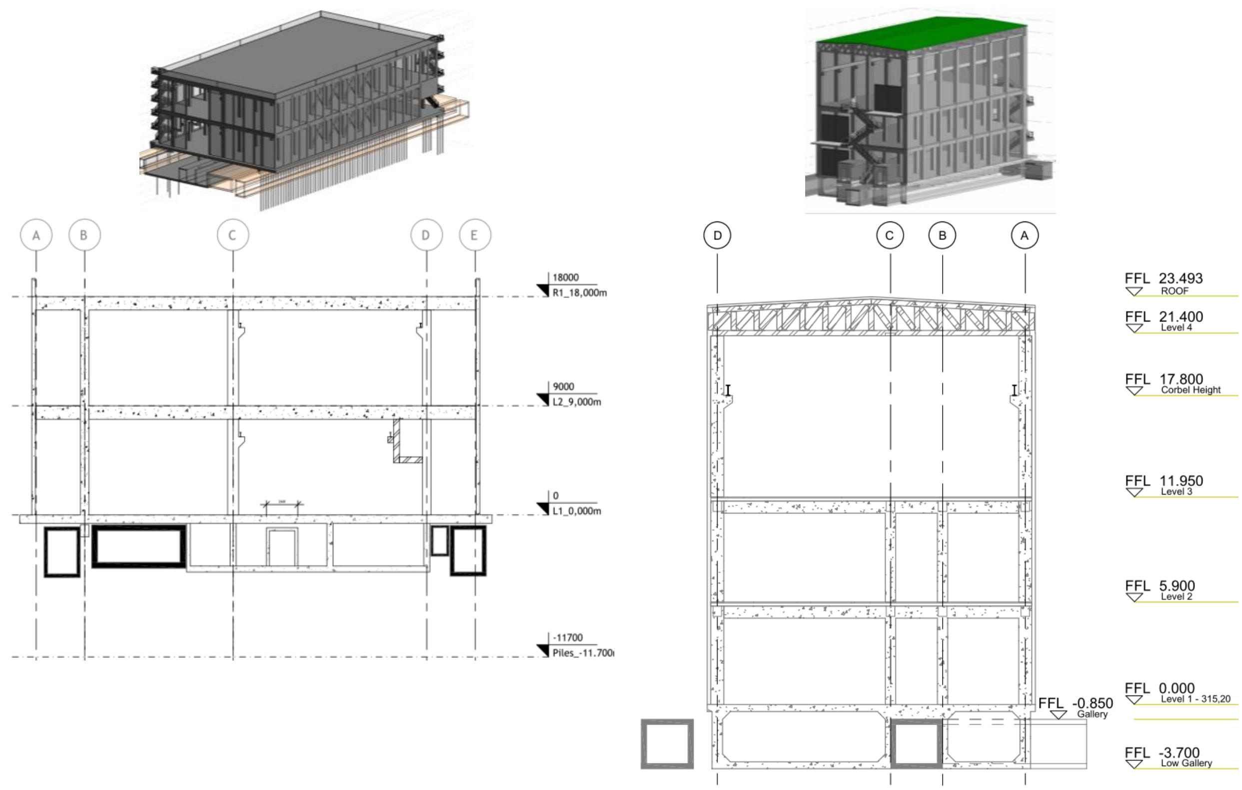

Dimensions: 37×66×22 (Width×Length×Height in meters)

- Level B1: - 4.000 m (Foundation slab)
- Level L1: + 0.000 m (Floor slab)
- Level L2: + 9.000 m (First level slab)
- Level R1: +18.000 m (Roof)

Dimensions: 17.5×35.7×27.193

- Level B1: - 3.700 m (Foundation slab)
- Level L1: + 0.000 m (Floor slab)
- Level L2: + 5.900 m (First level slab)
- Level L3: + 11.950 m (Second level slab)
- Level L4: + 21.400 m (Third level roof bottom)
- Level R1: + 23.493 m (Roof top)

Figure 1. Buildings #18 and #20 preliminary dimensions.

METHODOLOGY

Material properties

Material parameters for the buildings are taken in accordance with the I-SDCB and Eurocodes 2 and 8. Structural concrete strength is f_{ck} = 40 MPa (C40/50). Reinforcing steel characteristic strength is f_{yk} = 500 MPa (B500SD). The roof of Building #20 is made of Structural steel class S275. Soil properties are taken from the geotechnical study (I-SIR). Limestone rock is found at a depth of 4.00 m (bottom of existing galleries). Its static Young's modulus is 150 MPa, Poisson's ratio is 0.20, friction angle 30º, and no cohesion is considered.

Damping will be taken according to RG 1.61. For SL-2 (SSE) seismic events, ξ = 7% is adopted for concrete structures, while ξ = 4% is adopted for steel structures.

Behavior Factor concept

In Eurocode 8, the behavior factor q reflects a structure's capacity to dissipate energy through plastic deformation during seismic events. It allows for a reduction in the elastic response spectra, lowering design forces while ensuring adequate ductility and safety. The value of q varies based on the structural system, ductility class, and design approach. For reinforced concrete structures, q typically ranges from 1.5 to 4, depending on the structural system (moment-resisting frames, shear walls) and ductility class (low, medium, high). The reduced seismic forces for design are calculated as:

$$S_a = \frac{S_e}{q} \tag{1}$$

However, q is not constant across all frequencies. For high frequencies (short periods), a minimum q value (typically q = 1.50) ensures that the elastic response dominates in stiff structures. For low frequencies (long periods), the full energy dissipation potential is considered. Figure 2 presents the Horizontal (Vertical is obtained scaling by 2/3) Design Spectra (I-LSSR) for soft soils (left) and rock (right), with 7% damping and different values of q. Between period T = 0.1259 s (frequency 7.94 Hz) and T = 0.0294 s (frequency 34.00 Hz), the following interpolation is applied:

$$S_a(q,f) = \frac{S_e(f)}{q} + \left(\frac{S_e(f=34\ Hz)}{1,5} - \frac{S_e(f)}{q}\right) \cdot \frac{(f-7,94)}{(34-7,94)}; \quad 7.94 \leq f \leq 34\ Hz \tag{2}$$

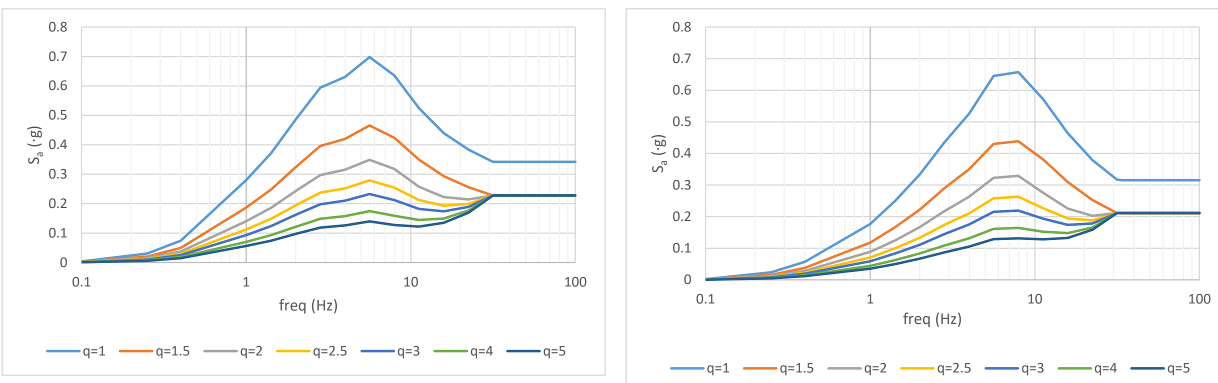

Figure 2. Horizontal Design Response Spectra and Behavior Factor. Soft soil (left), Rock soil (right)

Soil flexibility and strength

Soil stiffness is calculated using the Equivalent Elastic Half-Space Method. The equivalent bedding stiffness for Building #18 is k_{sz} = 10.75 MN/m^3, whereas for Building #20 it is k_{sz} =11.53 MN/m^3. Although both buildings share similar rock properties beneath the foundation, Building #18 is in a zone requiring soil replacement and is thus classified as soft soil for design.

Because no admissible soil pressures were provided as input data, classical formulations for rigid foundations (Bowles) were used to estimate soil bearing strength, which is considered acceptable for conceptual design purposes. The presence of underground galleries requires micropiles below alignments B, C, and D (see Figure 1). For this analysis, micropiles are sized according to classical methodologies (MFOM). To account for group effects, the stiffness of single piles is multiplied by 0.5 (horizontal) and 0.6 (vertical).

Finite Element Model

Finite element models were created using SAP2000 software, with beam elements representing columns, transverse walls, and beams in the plane models. The initial version of each model used fixed-base supports at ground-contact zones. In subsequent versions, soil stiffness—including micropile contributions—was modeled via spring elements. Non-structural mass was incorporated by assigning linearly distributed mass to the beam elements. Figure 3 shows the representative frame models for Buildings #18 (left) and #20 (right).

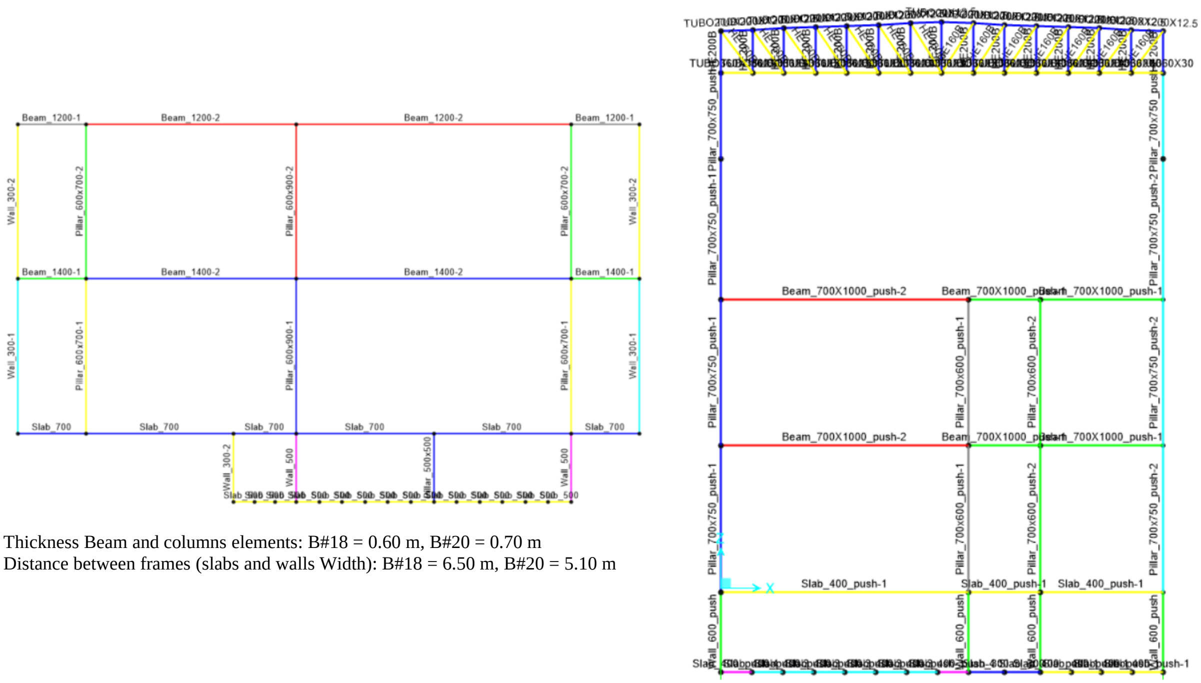

Figure 3. Frame FEM models for Buildings #18 and #20.

Preliminary design

Before conducting the pseudo-static (seismic) analysis, a conventional linear-elastic analysis was performed to verify the dimensions of the structural elements and calculate the required reinforcement. For conceptual design, three key load combinations are used: **SLS.qp** (Serviceability Limit State – quasi-permanent), **ULS.f** (Ultimate Limit State – frequent), and **ULS.e** (Ultimate Limit State – seismic). For the SLS load combination, the main goal is to check deformations. While cracking is often verified under SLS, it is not included here (tensile stresses can be assessed according to ITER standards), since the focus of this study is on ULS.e, the critical aspect required for assessment. Table 1 summarizes the relevant loads and combinations; the density of reinforced concrete is taken as 25 kN/m³.

After verifying displacements for the SLS.qp load combination, the design proceeds with ULS.f. Here, SAP2000's design module calculates the required reinforcement under frequent ultimate load conditions. The ULS.e combination then requires a modal spectral analysis (Response Spectrum Analysis). In line with RG 1.61, a damping ratio of $\xi = 7\%$ is used for concrete. Multiple design spectra are considered, varying with the behavior factor q. Values of q range from 1 to 4 for horizontal spectra and from 1 to 1.5 for vertical spectra (in accordance with Eurocode recommendations). A Newmark-type directional combination is employed, applying 100% of the horizontal load plus 40% of the vertical load, focusing on maximizing horizontal effects.

Table 1: Loads and Load Combination

SLS.qp	$Q_{SLS.qp} = 1.00\cdot(G_0 + G + G_{roof}) + 0.30\cdot(L + L_{roof})$	Dead Loads	Live Loads
ULS.f	$Q_{ULS.f} = 1.35\cdot(G_0 + G + G_{roof}) + 1.50\cdot(L + L_{roof})$	$G = 10$ kN/m^2	$L = 4$ kN/m^2
ULS.e	$Q_{ULS.e} = 1.00\cdot(G_0 + G + G_{roof}) + 0.50\cdot(L + L_{roof}) + 1.00\cdot E$	$G_{roof} = 3$ kN/m^2	$L_{roof} = 2$ kN/m^2

SAP2000's design module automatically combines the internal forces from the modal spectral analysis according to its internal combination rules (Table 2). This enables calculation of the required reinforcement for different *q* values. The final reinforcement selection covers the envelope of ULS.f and ULS.e combinations for each *q*.

Table 2: Combination rules for internal forces for beam elements in SAP2000.

Design Check	N (Axial Force)	V (Shear Force)	M (Bending Moment)
Compression (N)	-1	0	0
Tension (N)	+1	0	0
Shear Capacity (V)	0	+1 / -1	0
Positive Bending (M)	0	0	+1
Negative Bending (M)	0	0	-1
Interaction (N + M)	+1 / -1	0	+1 / -1

- *+1: Positive effect (e.g., tension for axial force, positive moment)*
- *-1: Negative effect (e.g., compression for axial force, negative moment)*
- *0: Not relevant for this design check*

Pushover Analysis

The pushover analysis methodology follows Eurocode 8 and involves applying incremental lateral loads to a structural model to assess its capacity under seismic conditions. The same finite element model is used, but nonlinear material properties—accounting for concrete and steel stress-strain curves per Eurocode 2—are introduced. Because the model uses beam elements, these nonlinearities appear only in the cross-sectional normal strains (Navier hypothesis), while shear-related nonlinearities are not directly included. Figure 4 shows the nonlinear constitutive equations for concrete (C40/50) and steel (B500S).

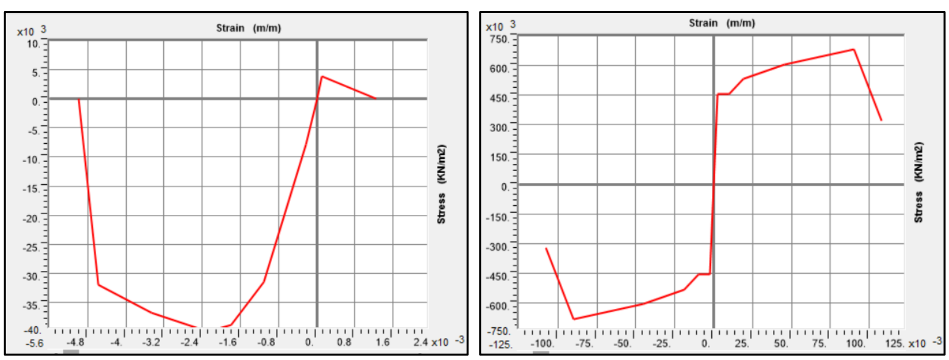

Figure 4. Non-linear constitutive equation for concrete (left) and steel (right)

Plastic Hinges

A key step is defining plastic hinges in SAP2000, which provides specific hinge assignment methods for beams, columns, and foundations.

Beams: two hinge configurations can be used: Equal Spacing and Nonlinear Beam-Column hinges,

- **Equal Spacing**: Hinges are distributed uniformly along the beam length, allowing inelastic behavior at multiple points but increasing computational effort.
- **Nonlinear Beam-Column Hinges**: Hinges are placed at beam ends (typically the outer 10% of the span), assuming plastic hinging at the ends. This method is more conservative and commonly used in practice.

SAP2000 can auto-define these hinges according to ASCE 41-17 (Table 10-7). For beams, the hinge properties typically consider bending (M3) and shear (V2), while neglecting axial force (N).

Columns: as with beams, columns can use equal spacing or end hinges. However, column hinges must consider axial-moment (P-M3) interaction, reflecting how axial loads affect ductility. Auto-defined hinges follow ASCE 41-17 (Table 10-8).

Foundations: These elements are usually modeled with springs rather than discrete hinges, since they do not form plastic zones like beams or columns. Continuous spring supports can capture nonlinear foundation response in compression (and zero tension resistance), ensuring realistic load-transfer modelling.

The use of ASCE 41-17 for defining plastic hinges ensures consistency with widely recognized standards for seismic evaluation. The hinge properties outlined in Tables 10-7 and 10-8 are derived from extensive experimental research and calibrated to reflect the typical performance of structural elements under seismic loads. This approach simplifies the modeling process while maintaining reliability across a broad range of applications. Although these parameters represent general conditions, they have been validated for use in practice, offering a robust framework for evaluating inelastic behavior in beams and columns. Their integration into SAP2000 allows for efficient and standardized hinge assignment, supporting accurate and code-compliant seismic performance assessments.

Figure 5 presents an example plastic hinge (Hinge 18H1) for Building #18 in SAP2000, showing moment-rotation (M–θ) relationships. These relationships are derived from material properties and cross-sectional dimensions, describing the structure's transition from elastic to inelastic behavior under increasing load.

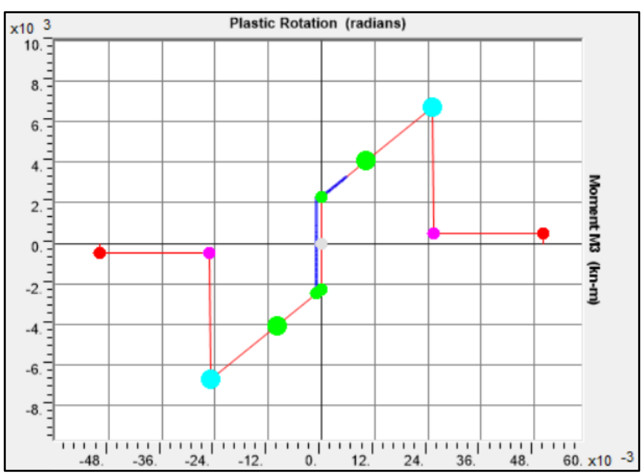

Figure 5. Example of Hinge 18H1 plastic state for Building #18 in SAP2000

Lateral Load Pattern

To define the lateral load Pattern, the following sub-steps are required:

- **Eigen value analysis** to obtain natural frequencies and mode shapes.
- **Selection of the main horizontal mode** to represent the primary seismic direction.
- **Definition of lateral forces**, as follows:

$$F_i = m_i \phi_i \tag{3}$$

where:

m_i = mass at level i

ϕ_i = amplitude of the first mode shape at level i

Gravity loads (permanent and variable) are also included to account for P-Δ effects.

Incremental Analysis

Once defined the load pattern that represent the seismic action, it is performed a non-linear analysis in which the loads are applied incrementally, and the resultant lateral displacement is monitored in a reference node located in the upper part of the building, and the opposite side of the side in which the lateral loads are applied (Betbeder-Matibet, J.). This implies a nonlinear static analysis at each load increment, where P-Delta effects are included, allowing for the formation of plastic hinges and redistribution of internal forces.

The curve Base Shear (V_b) vs. Top Displacement (Δ), or the “Capacity curve”, is the main result extracted from the analysis. It is important to monitor during the process the sequence of plastic hinge formations and their locations within the structure to understand the collapse process. Following the Annex B of Eurocode 8, this curve obtained from multi-degree-of-freedom (MDOF) system, it is converted into an equivalent single-degree-of-freedom (SDOF) system. This implies the following transformation factors (Urbanski A. et al.), that are obtained from the lateral modal shape used to define the lateral load pattern,

$$\Gamma = \frac{\sum_{i=1}^{n} m_i \phi_i}{\sum_{i=1}^{n} m_i \phi_i^2} \ ; \ M^* = \Gamma \cdot \sum_{i=1}^{n} m_i \phi_i \ ; \ d^* = \frac{\Delta}{\Gamma} \ ; \ F^* = \frac{V_b}{\Gamma} \tag{4}$$

Being, Γ: Modal participation factor, M^*: Modal mass, d^*: Effective displacement, F^*: Effective force. The SDOF curve will be generated from the effective capacity curve (F^* vs. d^*). The Eurocode propose a bi-linear curve that require to compute the energy E_m^* where the maximum capacity F_y^* it is reached (being the corresponding displacement d_m^*) from the plot F^* vs. d^*. The bilinear curve should intersect the capacity curve at 60% of the maximum base shear. This implies that the displacement d_y^* that determine the elastic limit it is given by,

$$d_y^* = 2 \cdot \left(d_m^* - \frac{E_m^*}{F_y^*} \right) \tag{5}$$

The period T^* of the SDOF system is given by,

$$T^* = 2\pi \cdot \sqrt{\frac{m^* d_y^*}{F_y^*}} \tag{6}$$

These parameters allow the computation of the **Capacity Spectrum**, which is defined by the curve d^* vs. $S_a(d^*)$, being,

$$d^* = \frac{\Delta}{\Gamma} \ ; \ S_a(d^*) = \frac{F^*(d^*)}{M^*} \tag{7}$$

The following step is the definition of the Demand Spectrum, in which the abscise of the design spectrum (Commonly defined by the period T) of the elastic design spectrum $S_e(T)$ is replaced by the following spectral displacement $S_d(T)$,

$$S_d(T) = \frac{T^2}{4\pi^2} S_e(T) \tag{8}$$

This converts the design spectrum in the format ADRS (Acceleration-Displacement Response Spectrum). Finally, the **performance point** is found in the intersection between both curves (Capacity vs Demand). The Eurocode 8 and the ATC-40 refine this first estimation in an iterative way, to calibrate the damping. In this paper, due the conceptual design point of view, the damping ratio is 7% and no iterations are performed. This point is determined based in the following procedure: the elastic Demand Spectrum is intersected by the linear-elastic Capacity Spectrum. For the same displacement, the ordinate of the non-linear Capacity Spectrum is determined. The behavior factor is estimated from the direct relationship between both quantities, equation 1.

It is important the verification of the structure seismic performance by ensuring the target displacement does not exceed the structure deformation limits. It is important that the inter-story drifts and the rotations in plastic hinges comply with some limitations to prevent excessive damage to non-structural elements. These limits are provided by the main regulations, for example, for Building #18, Eurocode 8 limits the maximum roof displacement to 0.22 m, that match the Immediate Occupancy (IO) limit defined by ASCE 41-17. The maximum roof displacement to Collapse Prevention (CP) is 0.55 m. On the other hand, for Building #20 the limit IO is 0.25 m, and the CP is 0.62 m.

RESULTS

The preliminary design following the linear elastic analysis, based in a reduced design spectrum. For Buildings #18 and #20, the reinforcement was determined for a range q = 1.5 to 2.0. For Building #18 the columns are considerably reinforced with steel ratios between 2.34% to 3.83%. The Beams elements have a symmetric reinforcement with steel ratios from 0.82% to 1.15%. For the Building #20 the column steel ratios vary between 1.31% to 2.30%, the beam steel ratios are between 0.57% to 1.15%. Other elements as walls and foundations have steel ratios from 0.39% to 0.82%. The volumetric reinforcement ratio for columns for Building #18 is in the range 6.40% to 8.76%, whereas for Building #20 is between 4.11% to 5.73%.

Figure 6 presents the pushover curves obtained from the non-linear analysis, the demand spectrum is presented for elastic response (blue) and q = 1.50 (brown). Red curves represent the MDOF system response, whereas the magenta curves the bilinear system determined according to Eurocode 8 specifications. The continuous lines are the capacity spectrum curves obtained from non-linear analysis, and the dashed lines the corresponding capacity curve obtained by means of linear-elastic analysis. As can be seen the behavior factor obtained from the MDOF responses are for Buildings #18 and #20 equals to 1.37, and 1.69, respectively. If the Eurocode bilinear curves are used, q equals 1.11, and 1.05. The difference between both estimations is found in the conservative approach used by Eurocode 8. On the other hand, the non-linear curves are still growing at the end of the plot, revealing that the collapse point is considerably distant from the performance point.

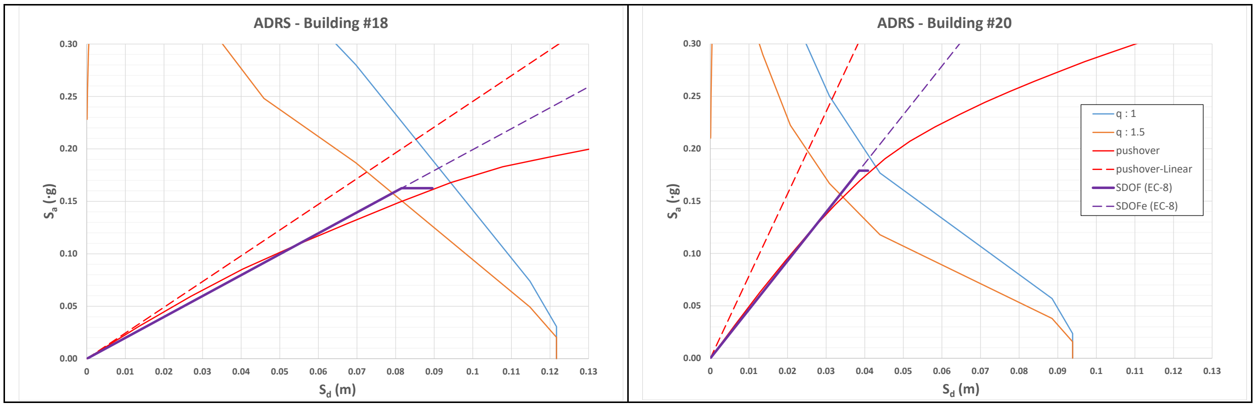

Figure 6. Pushover curves for Buildings #18 (left) and #20 (right).

CONCLUSIONS

The analyses conducted on Buildings #18 and #20 highlight significant differences in reinforcement demand and effective ductility. Building #18 requires considerably amount of column reinforcement, with steel ratios approaching 4%, compared to approximately 2% in Building #20. This disparity reduces the effective ductility of Building #18, largely due to structural irregularities, long spans subjected to non-seismic design loads, and geometric constraints imposed by underground galleries and existing structures.

The pushover analysis revealed that the actual behavior factor (q) is slightly lower than the assumed values but remains within an acceptable range. Furthermore, the performance point was consistently well separated from the collapse point, indicating a sufficient safety margin. However, the observed results suggest that for the specific conditions of these buildings, adopting a behavior factor exceeding 2 may not accurately reflect the structural response.

From a methodological perspective, the integration of nonlinear pushover analysis with conceptual design decisions proved instrumental in evaluating the seismic performance of these RC structures. The approach effectively captured critical aspects such as plastic hinge formation, capacity curves, and the interaction between ductility demands and reinforcement requirements. By incorporating considerations like load combinations, soil-structure interaction, and irregular geometries, the methodology provided a clear framework for addressing the unique challenges of nuclear facilities in seismic zones. However, some limitations remain, such as the exclusion of time-dependent dynamic effects, which could further refine the analysis in future studies.

To ensure reliable seismic performance for ITER project structures, particularly those characterized by high reinforcement demands, irregular geometries, and constrained load-transfer conditions, this study recommends limiting the behavior factor (q) to a maximum value of 2. This conservative limit aligns with the observed results, enhancing the robustness of the design and compliance with the stringent performance criteria required for nuclear facilities.

REFERENCES

ASCE 41-17: *"Seismic Evaluation and Retrofit of Existing Buildings,"* American Society of Civil Engineers (ASCE), Reston, VA.

ATC-40: *"Seismic Evaluation and Retrofit of Concrete Buildings,"* Applied Technology Council (ATC). 1996.

Betbeder-Matibet, J. *"Génie Parasismique - Prévention parasismique,"* volume 3. Hermes.

Bowles, Joseph E. *"Foundation Analysis and Design."* v5.0. The McGraw-Hill Companies, Inc.

Eurocode 8: "Design of Structures for Earthquake Resistance – Part 1: General Rules, Seismic Actions and Rules for Buildings (EN 1998-1)". European Committee for Standardization (CEN), Brussels.

Eurocode 2: *"Design of Concrete Structures – Part 1: General Rules and Rules for Buildings (EN 1992-1-1),"* European Committee for Standardization (CEN), Brussels.

I-SDCB. *"ITER Structural Design Code for Buildings (I-SDCB) - Part1: Design Criteria,"* IDM: 283B24 v3.0

I-LSSR. *"Load Specifications for Buildings with Safety Requirements,"* IDM: 2ERTXQ v3.3. ITER

I-SIR. *"ITER Project - Site Investigation Interpretative Report - Phase 1 and 2,"* IDM: 2M3XEC v1.3. ITER

MFOM. *"Guía para el Proyecto y la ejecución de micropilotes en obras de carretera."* Ministerio de Fomento de España, 2005.

RG 1.61: *"NRC Regulatory Guide on Damping Values for Seismic Design of Nuclear Power Plants, U.S. Nuclear Regulatory Commission."* U.S.NRC.

SAP2000 Structural Analysis Software, Version 25.1, Computers and Structures, Inc.

Urbanski A. et al. *"Static Pushover Analysis Report 070202,"* GeoDev. https://zsoil.com